

Future Prospects with *WMAP*

There is a theory which states that if ever anybody discovers exactly what the Universe is for and why it is here, it will instantly disappear and be replaced by something even more bizarre and inexplicable. There is another theory which states that this has already happened.

— Douglas Adams

The aim of science is not to open the door to infinite wisdom, but to set a limit to infinite error.

— Bertolt Brecht

1. Motivation

While *WMAP* has revealed the emergence of a standard cosmology, determining key cosmological parameters with unprecedented precision, it also leaves many unanswered questions that have dogged cosmologists for decades. The universe appears to consist of a bizarre mixture of cold dark matter (24%) and dark energy (71%), with the familiar baryonic matter that comprises everything we know being relegated to a mere 5%. What is dark matter? What is dark energy? What is the

inflaton? The answers to these classic questions are unknown. *WMAP* after one year provides tantalizing hints that the large angle power spectrum may contain surprises, and that the shape of the primordial power spectrum may not conform to expectations, but none of these hints provide definitive answers.

Some of these questions may have to await advances in theoretical cosmology and/or particle physics. However, the new *WMAP* results have shed light on a different type of uncertainty. While we can now clearly rule out cosmologies which predict grossly different CMB power spectra to the standard flat Λ CDM model with adiabatic initial conditions (e.g. defect models), it is still difficult to distinguish between models which are perturbations around this standard model. These models contain one or two extra parameters which seem only slightly favored at the $\leq 2\sigma$ level. It is important to develop quantitative statistical techniques which take into account the role of priors in order to distinguish between models which have roughly the same likelihood but differ by one or two extra parameters. One often resorts to Occam's Razor, which says that entities should not be multiplied without necessity, that is, the simplest explanation is preferred till the data demands a more complex model. Recent work seems to imply that this heuristic principle holds up under quantitative scrutiny; simple models seem indeed to be preferred by probability theory. We will briefly review two approaches to this problem that have appeared in the recent literature.

1.1. Bayesian Evidence

While the peak of the likelihood provides a mechanism to choose between different models with the same parameterization, it is not adequate for choosing between models which have different variables or different numbers of variables. The

concept of “Bayesian Evidence” (Drell et al., 2000; Saini et al., 2003) characterizes this choice in terms of the ratio of posterior Bayesian probabilities of the two models.

A model is a set of rules to predict data from a given set of parameters and a prior which quantifies the probabilities of the different parameter values in the absence of data, i.e. one’s assumptions, which may be based on theory (the universe is flat), logic ($\Omega_b > 0$), or based on knowledge of other data-sets ($0.3 \leq h \leq 1.0$). Let a pair of models be specified by the hypotheses A and B , which are parameterized by the sets $\{\alpha_i^A\}$ and $\{\alpha_j^B\}$ and where the number of parameters in the sets may be different. One wishes to know which of the hypotheses are most consistent with the data (D) and the priors (I). Then, using Bayes’s Theorem, the ratio of their posterior probabilities is given by

$$\Gamma_{AB} = \frac{P(A|D, I)}{P(B|D, I)} = \frac{P(A|I)}{P(B|I)} \times \frac{P(D|A, I)}{P(D|B, I)}, \quad (5-1)$$

where $P(A, I)$ is the probability of hypothesis A given the priors, and $P(D|A, I)$ is the likelihood of the data marginalized over all possible values of the parameters α_i^A given the priors. The latter term can be calculated directly from the output of the MCMC: it is effectively given by the ratio of likelihood maxima $\mathcal{L}_{max}(A)/\mathcal{L}_{max}(B)$. When Γ_{AB} is much larger than one, hypothesis A is preferred, which hypothesis B is preferred if Γ_{AB} is much smaller than one. If the ratio is of order 1, then there is no clear preference.

1.2. The Razor

Work by Balasubramanian (1996a,b); Myung et al. (2000) shows that the simplicity of a model family can be tied to geometric properties of the model seen as a subspace of the space of distributions. From a geometric perspective, a parametric model family of probability distributions forms a Riemannian manifold embedded

in the space of all distributions, described by a metric which can be taken to be the Fisher Information matrix. These authors define a measure of the complexity of a parametric distribution relative to a given true distribution, called the *razor* of a model family. Bayesian inference and the Minimum Description Length (MDL) principle (which states that the best model for describing a data set is the one that permits the greatest compression of the data description) are shown to give empirical approximations of the razor. The razor requires that the prior distribution must give equal weight to each *distinguishable* distribution indexed by the model parameters. Because the level of new notation and concepts that need to be introduced for a detailed description of the razor is not appropriate for this discussion, the reader is referred to the papers above for further details.

Further work needs to be done to apply this technique to likelihood surfaces obtained by MCMC, since in its current formulation there is an ambiguity in deciding what part of the phase volume to consider in the case where a prior on a given parameter is never hit by the Markov chain.

Leaving this topic for future work, we now consider how introducing extra parameters beyond the simplest model can bias parameter estimation. It is intuitively clear that when long, flat (i.e. models along the degeneracy have roughly the same likelihood) degeneracies in parameter space are present, especially for parameters where the degeneracy is not symmetric about the null or nominal value of the parameter (such as r , τ , and w), the mean values of other parameters (even those that are not part of the degeneracy) can be “pulled”. This is because marginalizing over the degeneracy surface will yield a mean value that is at its “center of mass”, and if there is more phase on one side of a nominal value than the other, the marginalized mean value will be on the side with greater phase space. For example, there is more phase space for $\Omega_{tot} > 1$ than $\Omega_{tot} < 1$ (see Fig. 3.13),

and so the mean Ω_{tot} yields a closed model, even though this drives means of some parameters away from their flat Λ CDM values (for example, the mean value of h is more than 1σ lower from the Λ CDM mean). Similarly, there is a lot more phase space for $w < -1$ than $w > -1$ (see Fig. 3.11), again resulting in a mean value that has $w < -1$ and pulling some other parameters (the mean of h is more than 1σ higher than its Λ CDM value). For the single field inflation case, one can explicitly see from Table 4.1 how far the other parameters have been pulled by the (n_s, r) degeneracy off the Λ CDM mean values in Table 3.7.

Thus, we can see that minimizing or breaking degeneracies is highly desirable for cosmological parameter estimation. Even simply narrowing the width of a long degeneracy direction can improve the consistency between the means of parameters that are not part of the degeneracy, when comparing two models where one contains the degeneracy and the other doesn't (for example, Λ CDM and w +CDM, where the latter contains an extra degeneracy between $[w, h]$ and $[w, \Omega_m]$). While one can break degeneracies by adding data sets which have different degeneracy directions from the CMB data set (e.g. large scale structure and supernova surveys), it is also true, at least for the foreseeable future, that these non-CMB analyses are complicated by systematic uncertainties that are significantly larger than for the CMB case, where systematics are well-understood and can be rigorously controlled by experimental design and analysis techniques. Thus, it is interesting to see what can be done to minimize degeneracies using the CMB alone, by using all the information present in the temperature, E- and B-mode polarization auto- and cross-correlation power spectra, as a function of the number of years WMAP could potentially be kept operating.

This chapter investigates three base cosmologies: (1) the standard Λ CDM model and a pair of models which perturb around it; (2) Λ CDM+running, and (3)

the “single-field-inflation” Λ CDM+running+tensors. The selected parameters for the base cosmologies are close to their respective maximum likelihood models found in the analysis of Chapters 3 and 4. The goal of this chapter is to evaluate the likelihood surfaces for these models assuming that *WMAP* continues operating for 4, 6 and 8 years and obtain reasonable estimates for the error bars one can expect for their respective parameters in each of the cases. As a by-product, we seek to discover effects (such as off-diagonal terms) that need to be included in the covariance matrix, and methodology that might reduce biases in parameter estimation in future *WMAP* analyses.

2. Creating Test Data

The cosmological parameters for the three base cosmologies are listed in Table 5.1. Figure 5.1 shows the base model for the power law Λ CDM case with the cosmic variance + noise errors after 4, 6 and 8 years for the TT , TE , EE and BB power spectra.

For each case, simulated Monte Carlo realizations of full sky CMB maps with white noise for Q, V and W channels were created, taking the noise bias n_ℓ^{TT} , $n_\ell^{EE} = 2n_\ell^{TT} = n_\ell^{BB}$ at the correct levels for the requisite number of years of operation. Basically, n_ℓ^{XX} for y years of operation is given by $[n_\ell^{XX}$ for 1 year of operation]/ y . A different Monte Carlo realization was used for each time-frame of operation, for each model. The maps were combined with N_{obs}^{TT} weighting (which is not optimal in all ℓ regimes, but is unbiased), the Kp2 sky cut was applied to the map, and the power spectra for C_ℓ^{TT} , C_ℓ^{TE} , C_ℓ^{EE} , C_ℓ^{BB} , C_ℓ^{TB} were estimated from the simulated maps. Since the last should be zero, it serves as a consistency check. Including C_ℓ^{BB} in models (1) and (2), which contain no tensor modes, also serves as

Table 5.1. Cosmological Parameters for Fiducial Models

Parameter	(1) Power Law Λ CDM	(2) Running Index Λ CDM	(3) Single Field Inflation
$\Omega_b h^2$	0.0238	0.0224	0.0235
$\Omega_m h^2$	0.144	0.135	0.134
n_s^a	0.99	0.93	1.13
τ	0.166	0.168	0.184
A^a	0.88	0.83	0.75
h	0.72	0.71	0.75
$dn_s/d \ln k$	—	-0.031	-0.055
r^b	—	—	0.41

^aDefined at $k=0.05 \text{ Mpc}^{-1}$ for models (1) and (2), and $k=0.002 \text{ Mpc}^{-1}$ for model (3).

^bDefined at $k=0.002 \text{ Mpc}^{-1}$.

a consistency check and lets us ascertain whether the covariance matrix requires the inclusion of additional effects.

For longer operation of *WMAP*, the covariances between the *TT*, *TE*, *EE* and *BB* become important. The diagonal part of the covariance matrix can be modeled as D_ℓ^{ij} where $\{i\}=\{TT, TE, EE, BB, TB, EB\}$. The covariance matrix is given by

$$\Sigma_{\ell\ell'}^{ij} = \sqrt{D_\ell^{ij} D_{\ell'}^{ij}} \left(\delta_{\ell\ell'}^K - r_{\ell\ell'}^{ij} \delta_{ij}^K \right) + \epsilon_{\ell\ell'}^{ij}, \quad (5-1)$$

where the definitions of $r_{\ell\ell'}$ and $\epsilon_{\ell\ell'}$ are the same as in Section 2.2. For ≥ 4 years *WMAP* operation, we set the beam uncertainties and point source subtraction errors to zero (i.e. $\epsilon_{\ell\ell'} = 0$). We only include off-diagonal terms due to the sky cut that couple different ℓ -modes for the diagonal terms Σ^{ii} . The curvature matrix is given by

$$Q_{\ell\ell'}^{ij} = D_\ell^{ij-1} \delta_{\ell\ell'}^K + \frac{r_{\ell\ell'}^{ij} \delta_{ij}^K}{\sqrt{D_\ell^{ij} D_{\ell'}^{ij}}}. \quad (5-2)$$

For the *TTTT* term, we use the likelihood approximation given in Eqs. 2-11 and 2-12, and for the other terms we use the Gaussian likelihood given by

$$-2 \ln \mathcal{L} = \sum_{ij} \sum_{\ell\ell'} \left(\mathcal{C}_{\ell'}^{i,\text{th}} - \hat{\mathcal{C}}_{\ell'}^i \right) Q_{\ell\ell'}^{ij} \left(\mathcal{C}_\ell^{j,\text{th}} - \hat{\mathcal{C}}_\ell^j \right). \quad (5-3)$$

In this analysis we have explicitly set to zero terms such as D_ℓ^{EBEB} , D_ℓ^{EEBB} , D_ℓ^{TTBB} etc, which are small, taking

$$D_\ell^{ij} \simeq \begin{pmatrix} D_\ell^{TTTT} & D_\ell^{TTTE} & D_\ell^{TTEE} & 0 & 0 \\ D_\ell^{TTTE} & D_\ell^{TETE} & D_\ell^{TEEE} & 0 & 0 \\ D_\ell^{TTEE} & D_\ell^{TEEE} & D_\ell^{EEEE} & 0 & 0 \\ 0 & 0 & 0 & D_\ell^{BBBB} & 0 \\ 0 & 0 & 0 & 0 & D_\ell^{TBTB} \end{pmatrix}, \quad (5-4)$$

but such terms can easily be included in future analyses. The various diagonal terms (in ℓ space) are given by

$$D_\ell^{TTTT} = \langle TTTT \rangle - \langle TT \rangle^2$$

$$= \frac{2(\mathcal{C}_\ell^{TT,\text{th}} + \mathcal{N}^{TT})^2}{(2\ell + 1)f_{sky}^2} \quad (5-5)$$

$$\begin{aligned} D_\ell^{TEETE} &= \langle TEETE \rangle - \langle TE \rangle^2 \\ &= \frac{(\mathcal{C}_\ell^{TT,\text{th}} + \mathcal{N}^{TT})(\mathcal{C}_\ell^{EE,\text{th}} + \mathcal{N}^{EE}) + (\mathcal{C}^{TE,\text{th}})^2}{(2\ell + 1)f_{sky}^2} \end{aligned} \quad (5-6)$$

$$\begin{aligned} D_\ell^{TTTE} &= \langle TTTE \rangle - \langle TT \rangle \langle TE \rangle \\ &= \frac{(\mathcal{C}_\ell^{TT,\text{th}} + \mathcal{N}^{TT}) \mathcal{C}^{TE,\text{th}}}{(2\ell + 1)f_{sky}^2} \end{aligned} \quad (5-7)$$

$$\begin{aligned} D_\ell^{EEEE} &= \langle EEEE \rangle - \langle EE \rangle^2 \\ &= \frac{2(\mathcal{C}_\ell^{EE,\text{th}} + \mathcal{N}^{EE})^2}{(2\ell + 1)f_{sky}^2} \end{aligned} \quad (5-8)$$

$$\begin{aligned} D_\ell^{TTEE} &= \langle TTEE \rangle - \langle TT \rangle \langle EE \rangle \\ &= \frac{(\mathcal{C}_\ell^{TE,\text{th}})^2}{(2\ell + 1)f_{sky}^2} \end{aligned} \quad (5-9)$$

$$\begin{aligned} D_\ell^{TEEE} &= \langle TEEE \rangle - \langle TE \rangle \langle EE \rangle \\ &= \frac{(\mathcal{C}_\ell^{EE,\text{th}} + \mathcal{N}^{EE}) \mathcal{C}^{TE,\text{th}}}{(2\ell + 1)f_{sky}^2} \end{aligned} \quad (5-10)$$

$$\begin{aligned} D_\ell^{BBBB} &= \langle BBBB \rangle - \langle BB \rangle^2 \\ &= \frac{2(\mathcal{C}_\ell^{BB,\text{th}} + \mathcal{N}^{BB})^2}{(2\ell + 1)f_{sky}^2} \end{aligned} \quad (5-11)$$

$$\begin{aligned} D_\ell^{TBTB} &= \langle TBTB \rangle - \langle TB \rangle^2 \\ &= \frac{(\mathcal{C}_\ell^{TT,\text{th}} + \mathcal{N}^{TT})(\mathcal{C}_\ell^{BB,\text{th}} + \mathcal{N}^{BB})}{(2\ell + 1)f_{sky}^2}, \end{aligned} \quad (5-12)$$

where $f_{sky} = 0.85/\sqrt{1.14}$, the numerator coming from the Kp2 sky cut and the denominator from the N_{obs}^{TT} weighting.

3. Parameter Estimation Results

We now carry out parameter estimation using MCMC for each of the models (1), (2) and (3). The results are presented below.

3.1. Λ CDM Model

Table 5.2 gives the results of the parameter estimation for the Λ CDM model for 4, 6 and 8 years, respectively. Figure 5.2 shows the 1-dimensional likelihood profiles for the model parameters for 8 years of operation - 4 and 6 year likelihood profiles look very similar. The mean recovered parameters fluctuate up and down by 1σ roughly a third of the time, as expected. But the table shows that τ and A are consistently biased higher than the fiducial values in parameter estimation from all three Monte Carlo realizations. Figure 5.3 shows the reason; by 4 years of operation, the τ vs n_s degeneracy is broken, and the dominant degeneracy is between τ and A . This degeneracy is important even after 8 years of operation, and is dependent on the position of the pivot point of the primordial power spectrum (see Figure 5.4). This suggests that the pivot point should be chosen with care to minimize this degeneracy, perhaps around $k = 0.02 \text{ Mpc}^{-1}$.

3.2. Running Index Λ CDM Model

Table 5.3 gives the results of the parameter estimation for the running scalar index model for 4, 6 and 8 years, respectively. While most of the recovered parameters show consistency, n_s , $dn_s/d \ln k$, τ and h show some biases in the 4 and 6 year analysis. This can again be attributed to the effect of degeneracies. By 8 years of operation, the degeneracies are smaller and the input parameters are recovered well. Figure 5.5 shows the degeneracies of τ , n_s and $dn_s/d \ln k$ which still exist after 8 years. The extra degeneracy of n_s vs. $dn_s/d \ln k$ over the Λ CDM model accounts for the fact that the error on n_s for the running index model does not improve to the level it does in the Λ CDM model.

It appears that if one is attempting to constrain models with a running spectral

Table 5.2. Estimated Parameters for Λ CDM Model

Parameter	4 Years	6 Years	8 Years	Fractional Error
$\Omega_b h^2$	0.0237 ± 0.0007	0.0248 ± 0.0007	0.0234 ± 0.0006	2.5%
$\Omega_m h^2$	0.138 ± 0.007	0.139 ± 0.006	0.144 ± 0.005	3.5%
n_s^a	0.98 ± 0.02	1.02 ± 0.02	0.988 ± 0.016	2%
τ	0.202 ± 0.020	0.198 ± 0.019	0.196 ± 0.016	10%
A^a	0.92 ± 0.04	0.93 ± 0.04	0.94 ± 0.03	3%
h	0.74 ± 0.03	0.76 ± 0.03	0.69 ± 0.02	3%
Ω_m	0.26 ± 0.03	0.24 ± 0.03	0.30 ± 0.03	11%

^aDefined at $k=0.05 \text{ Mpc}^{-1}$.

Table 5.3. Estimated Parameters for Running Index Λ CDM Model

Parameter	4 Years	6 Years	8 Years
$\Omega_b h^2$	0.0236 ± 0.0008	0.0248 ± 0.0009	0.0223 ± 0.0007
$\Omega_m h^2$	0.121 ± 0.007	0.122 ± 0.007	0.133 ± 0.006
n_s^a	1.00 ± 0.04	1.03 ± 0.04	0.94 ± 0.03
τ	0.199 ± 0.021	0.188 ± 0.019	0.199 ± 0.015
$dn_s/d \ln k$	0.025 ± 0.023	0.030 ± 0.027	-0.019 ± 0.021
A^a	0.85 ± 0.04	0.84 ± 0.04	0.88 ± 0.03
h	0.79 ± 0.04	0.81 ± 0.04	0.70 ± 0.03

^aDefined at $k=0.05 \text{ Mpc}^{-1}$.

index, especially if one does not have the luxury of running the *WMAP* experiment for 8 years, it is imperative to add data at small scales so as not to bias the recovered parameters. Having a well-constrained anchor point at small scales eliminates the extra degeneracies caused by $dn_s/d \ln k$. For instance, one can use data from ground-based CMB experiments, calibrated to the *WMAP* map, for this purpose. Even at 8 years' *WMAP* operation, while other parameters are not biased, one does not obtain a significant constraint on $dn_s/d \ln k$ unless it is much larger than the value specified here, -0.03 . But it is quite likely that a running index of this magnitude can be detected at 3σ by adding smaller scale data.

3.3. “Single Field Inflation” Model

Table 5.4 gives the results of the parameter estimation for the “single field inflation” model for 4 and 8 years, respectively.

The 4-year operation case still contains degeneracies which bias the recovered parameters significantly. Figure 5.6 shows that the degeneracy surfaces in the $(r, n_s, dn_s/d \ln k)$ planes are still significant (compare with Figure 4.3).

The 8-year operation case recovers the input parameters quite well. Figure 5.7 shows how much the degeneracy surfaces in the $(r, n_s, dn_s/d \ln k)$ planes have tightened (compare with Figure 4.3). It appears that if the level of tensor modes is as high as in this model (~ 0.4), a 3σ detection is possible after 8 years of *WMAP* operation. Again, adding smaller scale CMB data calibrated to *WMAP* should tighten constraints significantly.

3.4. Results in the (w, Ω_m) and (w, h) Planes

We explore the (w, Ω_m) and (w, h) degeneracies using the simulated data from the Λ CDM model, Model (1) above. We carry out parameter estimation using MCMC for a model with a constant equation of state, using parameters $[\Omega_b h^2, \Omega_m h^2, n_s, \tau, A, h, w]$. We assume 8 years of WMAP operation in this calculation. Figure 5.8 shows the constraints obtained on these planes, which, when compared with Figure 3.11, shows that the degeneracy has tightened especially for $w > -1$. The degeneracy surface is bi-modal. The τ vs. $\Omega_m h^2$ joint likelihood surface is also bi-modal for this model, which suggests that the degeneracy is being partially broken by the improvement in the polarization data.

3.5. Results in the $(\Omega_\Lambda, \Omega_m)$ Plane

Finally, we explore the $(\Omega_\Lambda, \Omega_m)$ degeneracy, again using the simulated data from the flat Λ CDM model. We carry out parameter estimation using MCMC for a non-flat model with the parameters $[\Omega_b h^2, \Omega_m h^2, \Omega_\Lambda, n_s, \tau, A, h]$. We assume 4 and 8 years of WMAP operation in this calculation.

Figure 5.9 shows how far the constraint has tightened compared to the constraint from the first year data (Figure 3.13). Table 5.5 shows that the constraint obtained from 8 years is not a significant improvement over 4 years.

4. Conclusions

The first year WMAP analysis was carried out with a level of rigor and care in order to do justice to the precision of the data. However, it is the first word on WMAP, not the last. It goes without saying that one must continue to

Table 5.4. Estimated Parameters for “Single-Field Inflation” Model

Parameter	4 Years	8 Years
$\Omega_b h^2$	0.0256 ± 0.0011	0.0238 ± 0.0007
$\Omega_m h^2$	0.119 ± 0.008	0.129 ± 0.006
n_s^a	1.06 ± 0.08	1.12 ± 0.05
τ	0.215 ± 0.019	0.216 ± 0.014
$dn_s/d \ln k$	-0.006 ± 0.038	-0.041 ± 0.022
r^a	0.75 ± 0.23	0.56 ± 0.15
A^a	0.75 ± 0.06	0.79 ± 0.05
h	0.85 ± 0.05	0.75 ± 0.03

^aDefined at $k=0.002 \text{ Mpc}^{-1}$.

Table 5.5. Estimated Constraints for Ω_{tot}^a

	4 Years	8 Years
Ω_{tot}	0.981 ± 0.009	0.993 ± 0.014

^aFlat Λ CDM fiducial cosmology from Table 5.1

improve the level of accuracy of both the covariance matrix and the parameter estimation/likelihood analysis. In this chapter we have investigated how parameter estimation can be biased by the presence of degeneracy surfaces in the likelihood. It is clear that the minimization of degeneracy directions is required in order to trust the mean values of parameters, given the continually improving quality of the data. Recommendations for future *WMAP* analyses based on these simulated parameter estimations are as follows:

1. Use the full covariance matrix between the possible combinations of power spectra. The *EEBB* and *EBEB* terms, which were neglected in this analysis, should also be included, since they influence the covariance of τ which still appears to be degenerate with another parameter to a small extent even in the 8 year data.
2. The pivot point of the primordial power spectrum in parameter estimation should be selected with great care to minimize degeneracies. A selection of pivot points should be tried to determine the best position to use.

There is no significant improvement in determining the parameters of a Λ CDM universe by extending the operation of *WMAP* to 6 or 8 years. However, the improvement in longer term operation is significant in constraining models with one or two extra parameters. We find that certain parameters of more complicated models are biased because of the existence of degeneracies. These could potentially be minimized or eliminated by operating *WMAP* for up to 8 years. In the case of a model with a running index, the degeneracies mainly occur because errors on small-scale fluctuations are too large; therefore it is likely that the same effect as operating *WMAP* for longer can be achieved by combining *WMAP* data with ground-based CMB experiments that measure high- ℓ models accurately, calibrated

to WMAP. In the case of a model with a high level of tensor modes (we have investigated $r \sim 0.4$), a 3σ detection of tensor modes is possible after 8 years. The constraints on flatness do not improve significantly when running WMAP for 4 vs. 8 years. The WMAP 8 year constraint on w , when combined with results from next generation supernovae experiments (e.g. *SNAP*, <http://snap.lbl.gov/>) can yield tight limits on the equation of state of dark energy, assuming that the systematic uncertainties in the future supernova data can be controlled to be of the same level as their statistical uncertainties.

We have mentioned that the combination of WMAP with smaller scale CMB experiments (for example, the next-generation version of the *BOOMERanG* experiment, <http://oberon.roma1.infn.it/boomerang/b2k/>, and future ground-based experiments) can significantly improve the science return of a longer-lived WMAP experiment for non-minimal- Λ CDM cosmologies. Calibrating a smaller scale experiment to WMAP can significantly improve calibration uncertainties in the small-scale experiment and hence improve the parameter constraints. The calibration uncertainty is minimized the closer WMAP is to being cosmic-variance-limited in the region of overlap between the two experiments. The cosmic variance limit of WMAP is $\ell \sim 495$ (4 years), $\ell \sim 545$ (6 years), and $\ell \sim 570$ (8 years). Thus, the longer WMAP runs, the better the science return will be from combining its data with small-scale experiments.

We have shown that it is very important to minimize degeneracy directions in a given model for the unbiased recovery of cosmological parameters. The improvements in the data (especially in the polarization data) gained by running the WMAP data for longer will significantly increase its power to distinguish among models which are perturbations about the standard “minimal” Λ CDM model. One can improve constraints further by adding smaller-scale ground-based CMB experiments

calibrated to the *WMAP* maps, and this calibration uncertainty decreases with the length of time *WMAP* continues operating.

We conclude by reiterating that great care must be taken when fitting models with parameters which have one or more flat degeneracy directions for a given data-set. For example, if one attempts to simultaneously constrain the usual FRW+primordial cosmological parameters [$\Omega_b h^2$, $\Omega_m h^2$, τ , h , n_s , A] plus Ω_Λ , w , $dn_s/d\ln k$ and r , with projected CMB data, one is likely to recover cosmological parameters which are biased due to the many degeneracies inherent between these parameters. An independent $\sim 1\%$ determination of the Hubble parameter with minimal systematics is likely to do much more for our ability to simultaneously constrain this parameter set than large improvements to CMB data over what will be achieved in the next few years. Unfortunately, this may not be a realistic goal, at least using present methods. However, given the formidable array of experiments planned for the next couple of decades, using a wide range of methods (CMB polarimetry, space-based interferometry, gravity wave detectors, the successor to the HST, particle accelerators, neutrino experiments, large scale structure surveys, and supernova surveys) as well as advances in numerical and statistical techniques, we may look forward to significant advances in our knowledge of the cosmos.

I acknowledge the hospitality of the Aspen Center for Physics, where much of this work was carried out, and Antony Lewis, Manoj Kaplinghat, Lloyd Knox, Olivier Dore, Yun Wang, Pia Mukherjee and Robert Crittenden for useful conversations on parameter estimation.

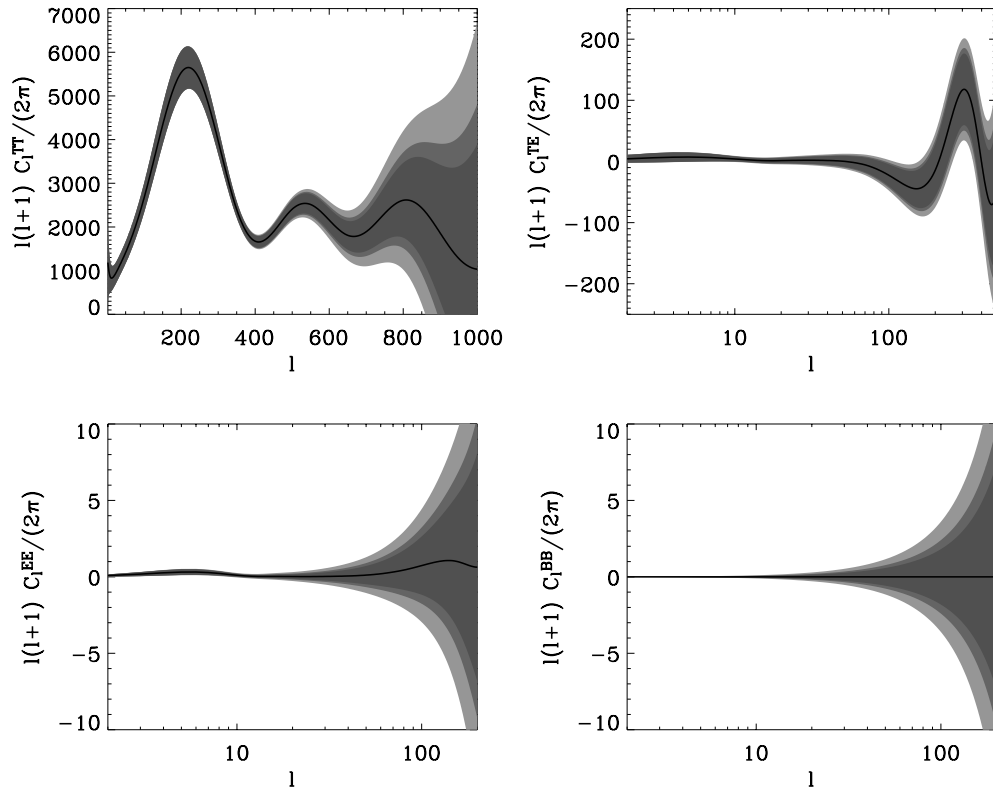


Fig. 5.1.— The base model (black line) for the power law Λ CDM case with the cosmic variance + noise errors after 4 (light gray band) , 6 (medium gray band) and 8 (dark gray band) years for the TT (top left), TE (top right), EE (bottom left) and BB (bottom right) power spectra.

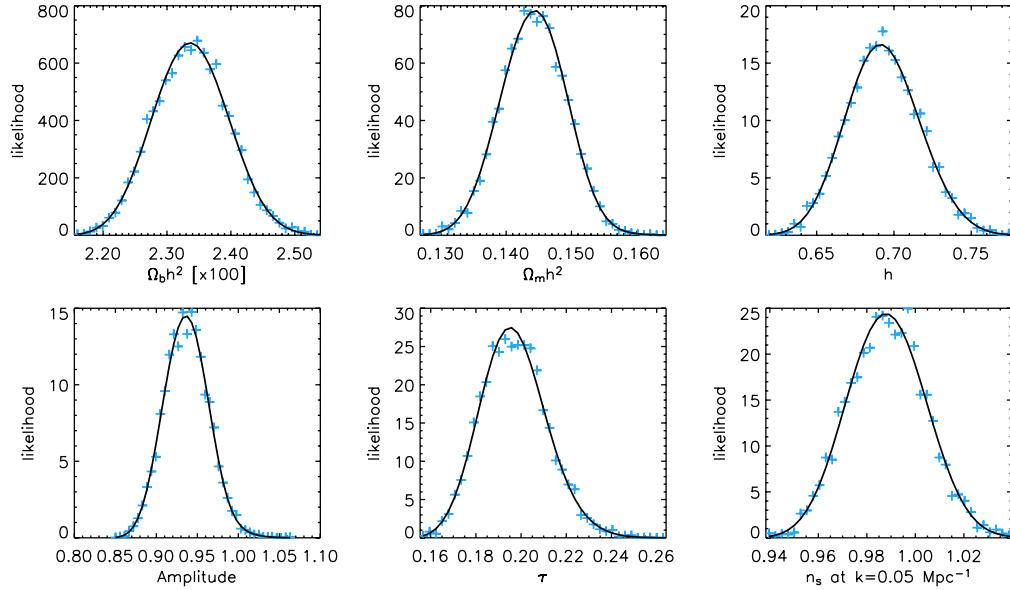


Fig. 5.2.— One dimensional marginalized likelihood profiles for the Λ CDM model after 8 years of WMAP operation. The likelihood profiles for 4 and 6 years do not differ significantly from this plot.

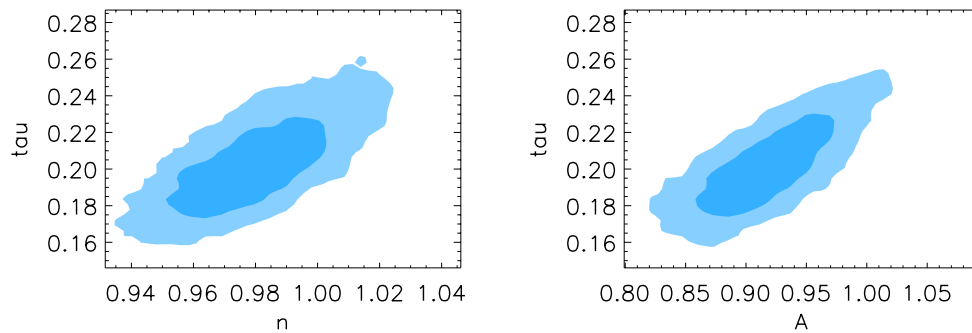


Fig. 5.3.— n_s vs τ and A vs τ joint likelihood surfaces for Λ CDM model after 4 years of WMAP operation. The likelihood surfaces for 6 and 8 years do not differ significantly from this plot.

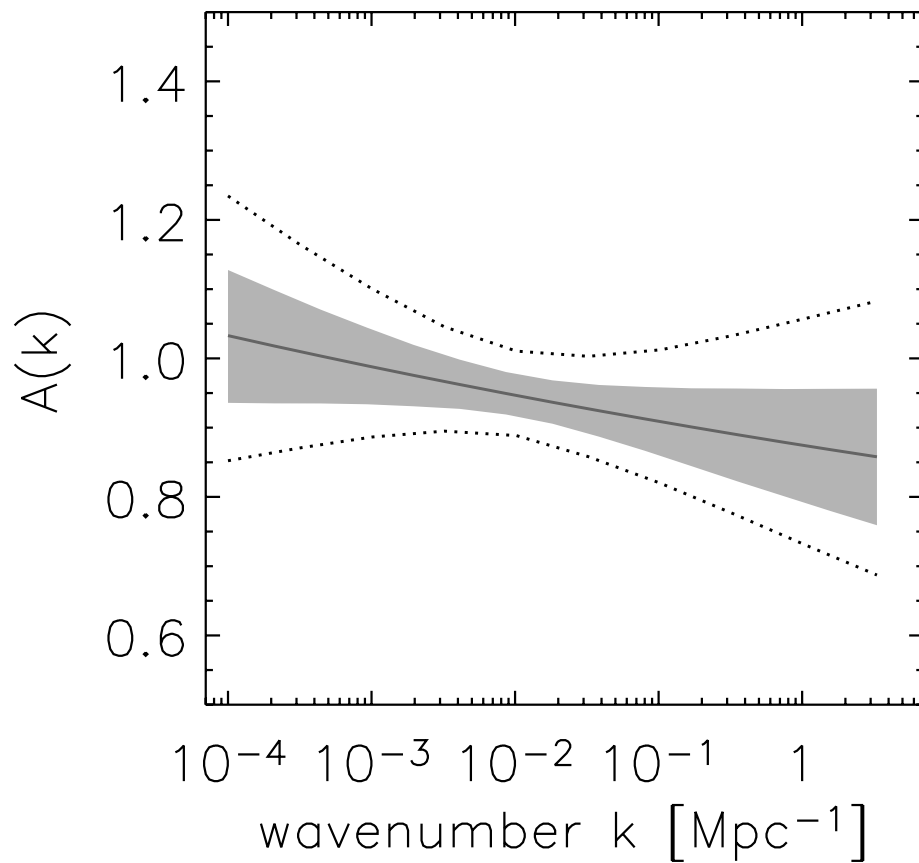


Fig. 5.4.— The amplitude parameter A as a function of k for 4 years of WMAP operation for the Λ CDM model. The solid line gives the mean value. The shaded area shows 68% errors and the dotted lines give the 95% errors. The constraints for 6 and 8 years do not differ significantly from this plot.

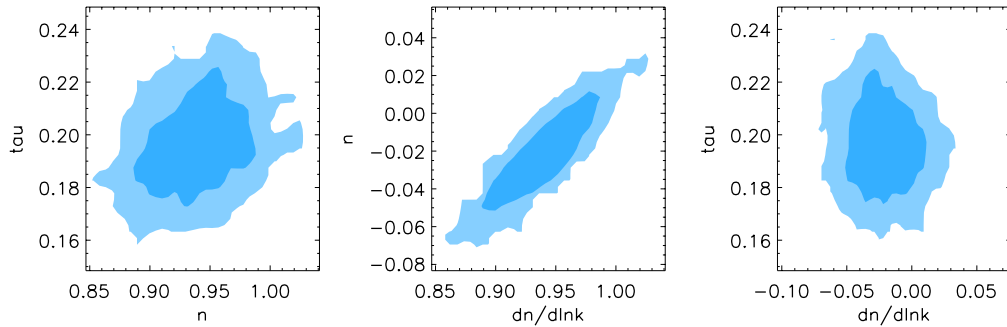


Fig. 5.5.— The 2-dimensional joint likelihood planes for τ vs. $(n_s, dn_s/d \ln k)$ for the running index model. The shaded area shows 68% errors and the dotted lines give the 95% errors. The degeneracy surfaces for 4 and 6 years are somewhat worse than in this plot.

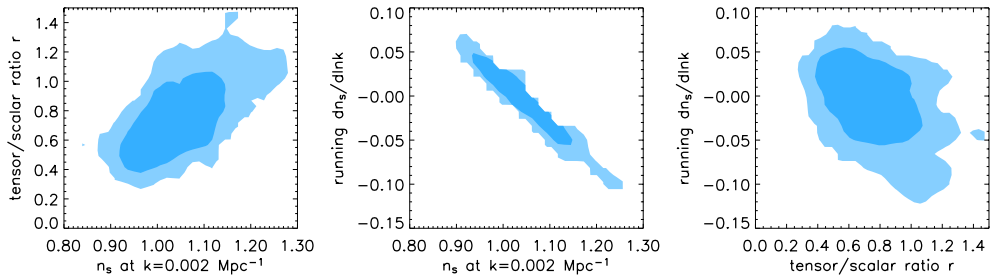


Fig. 5.6.— The 2-dimensional joint likelihood planes for $(r, n_s, dn_s/d \ln k)$ for the “single field inflation” model; the 68% confidence region (dark blue) and the 95% confidence region (light blue) are shown for 8 years of WMAP operation.

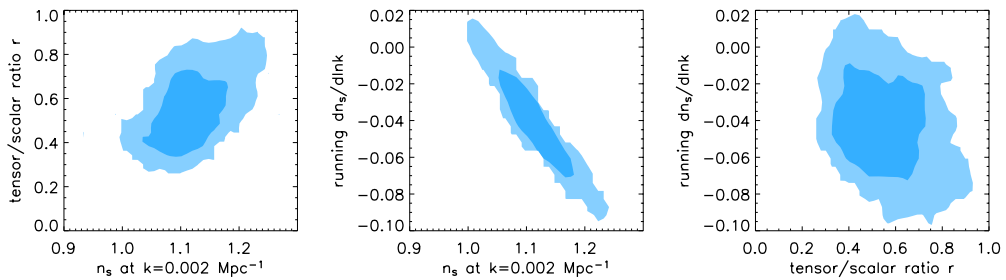


Fig. 5.7.— The 2-dimensional joint likelihood planes for $(r, n_s, dn_s/d \ln k)$ for the “single field inflation” model; the 68% confidence region (dark blue) and the 95% confidence region (light blue) are shown for 8 years of WMAP operation.

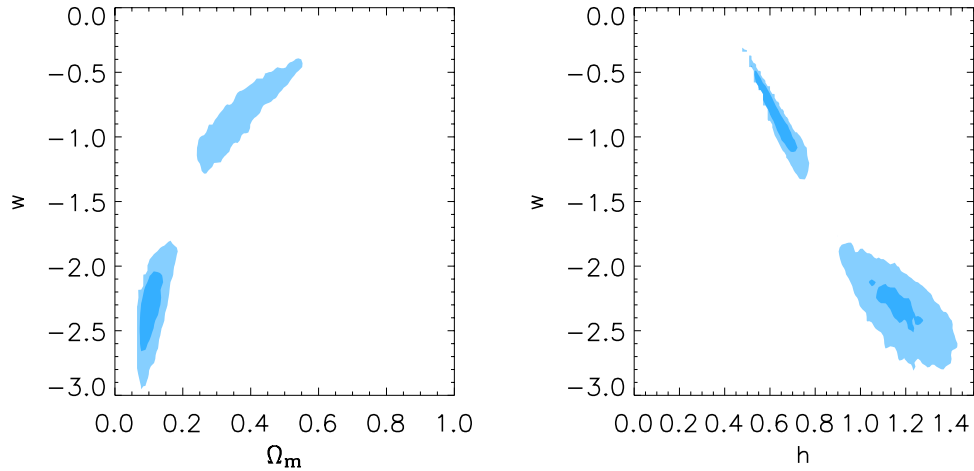


Fig. 5.8.— The 2-dimensional joint likelihood planes for (Ω_m, w) and (h, w) planes, using the Λ CDM model as the base cosmology; the 68% confidence region (dark blue) and the 95% confidence region (light blue) are shown for 8 years of WMAP operation.

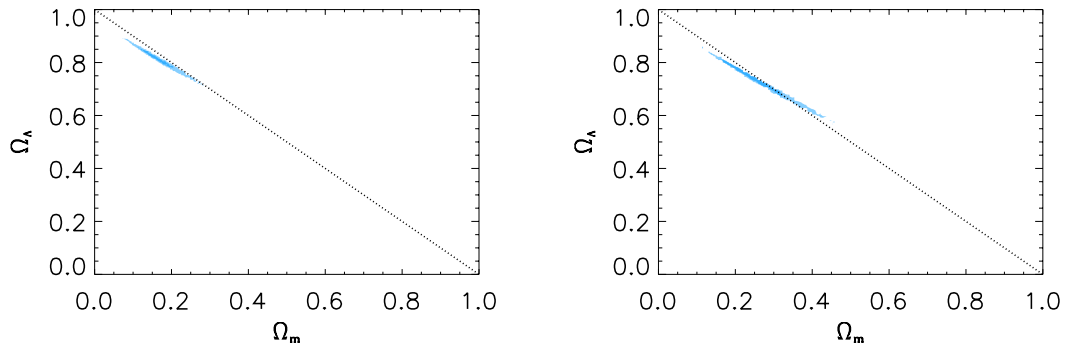


Fig. 5.9.— The 2-dimensional joint likelihood plane for the $(\Omega_m, \Omega_\Lambda)$ plane, using the Λ CDM model as the base cosmology; the 68% confidence region (dark blue) and the 95% confidence region (light blue) are shown for 4 (left panel) and 8 (right panel) years of WMAP operation.

Bibliography

Balasubramanian, V. 1996, adap-org/9601001

Balasubramanian, V. 1996, cond-mat/9601030

Drell, P. S., Loredo, T. J., Wasserman, I. 2000, ApJ, 530, 593

Myung, I. J., Balasubramanian, V., & Pitt, M. 2000, Proceedings of the National Academy of Sciences, 97, 11170

Saini, T. D., Weller, J., & Bridle, S. L. 2003, astro-ph/0305526